Hydrolytic products of diphthalimidodiethylamine and temperature independent sensitized luminescence of their lanthanide(III) complexes

Dawn M. Y. Barrett,[a] Ishenkumba A. Kahwa,*[,a] Bernd Radüchel,[b] Andrew J. P. White[c] and David J. Williams[c]

[a] *Chemistry Department, University of the West Indies, Mona, Kingston 7, Jamaica*
[b] *Forschung Kontrastmittel für Kernspinomographic Chemie, Schering Aktiengesellschaft Diagnostika, 13342 Berlin, Germany*
[c] *Chemical Crystallography Laboratory, Department of Chemistry, Imperial College of Science, Technology and Medicine, South Kensington, London, UK SW7 2AY*

Syntheses and structural and luminescence studies of hydrolytic products of diphthalimidodiethylamine (DPDA) and their lanthanide(III) compounds have been undertaken in order to determine the potential for the phthalamate functionality to sensitize intense Eu^{3+} and Tb^{3+} emission *via* the '*antenna effect*'. Acid promoted hydrolysis of the relatively simple DPDA is efficient; hydrolysis is negligible at pH > 11. At pH 2–3, hydrolysis to phthalic acid (1) occurs which upon interaction with DPDA yields the phthalic acid–DPDA supramolecular hydrate, DPDAH–HP·1.75H_2O. With a potassium carbonate–ethanol–acetonitrile mixture containing a small amount of water, the novel phthalamate–phthalimide H2·H_2O is formed while at pH *ca.* 9–10 the new diphthalamate $Na_2$3·3H_2O is formed. These transformations have been confirmed by single crystal X-ray analyses of DPDAH–HP·1.75H_2O and H2·H_2O. The crystal structures of DPDAH–HP·1.75H_2O and H2·H_2O reveal that the phthalamates and phthalimides are stabilized by non-covalent (*e.g.* π–π stacking and hydrogen bonding) interactions which are of interest as potential conduits for energy transfer and are responsible for molecular aggregations seen in FAB mass spectrometry of H2·H_2O and $Na_2$3·H_2O. Europium(III) compounds of 3^{2-} and H2 exhibit intense sensitized red emission which is, surprisingly, temperature independent.

There is currently considerable interest in new types of organo-chromophosphors capable of sensitizing intense red and green emission from europium(III) [$Eu^{3+}(^5D_0)$] and terbium(III) [Tb^{3+}-$(^5D_4)$] respectively.[1–10] Emission from these cations is usually weak because the electronic transitions involved are forbidden.[11] But emission strong enough to be considered for use in biomedical diagnostic agents may be obtained by suitable coupling between electronic states of organo-chromophores and those of the rare earth ions (Ln^{3+}) in which ligand-to-metal energy transfer, '*the antenna effect*',[1–10] is efficient. Because of our interest in phthalimides as preparative intermediates[12,13] and their broad emission in the visible region (400–600 nm)[14] which overlaps with key lanthanide(III) electronic absorptions, such as $^5D_J \leftarrow {}^7F_{J'}$ ($J = 0$, $J' = 0$ for Eu^{3+} and $J = 4$, $J' = 6$ for Tb^{3+}),[15] we have explored the potential for the phthalimide and phthalamate functionality to bind to lanthanide(III) cations with a concomitant '*antenna effect*'. Our interest in these systems was inspired by the ease with which phthalates and phthalimides engage in extended intermolecular interactions,[12,13] which we find to be attractive as potential conduits for electronic excitation energy. In order to determine whether the desired lanthanide(III) cation binding and coupling to phthalimides and phthalamates are achievable we studied the behaviour of a relatively simple diphthalimidodiethylamine (**DPDA**) and its phthalamate derivatives, the carboxylate group of which is a potentially better lanthanide(III) complexing agent.[16]

Herein we report the preparation of the new supramolecular complex of **DPDA** with phthalic acid (**1**) (**DPDAH–HP·1.75H_2O**), zwitterionic phthalimide–phthalamate **H2·H_2O** and bisphthalamate **$Na_2$3·3H_2O** as well as the crystal structures of **H2·H_2O** and **DPDAH–HP·1.75H_2O** and luminescence characteristics of Eu^{3+} and Tb^{3+} complexes of **H2** and $\mathbf{3}^{2-}$.

Results and discussion

Hydrolysis and crystallography

The essential features of the pH dependent[17,18] hydrolytic reactions are summarized in Scheme 1. Under acidic conditions complete hydrolysis of the phthalimide functionality to phthalic acid, which upon reaction with **DPDA** produces a stable complex, **DPDAH–HP·1.75H_2O**, dominates. Hydrolysis under mildly basic conditions with potassium carbonate in an acetonitrile–ethanol mixture containing small amounts of water yields a novel phthalimide–phthalamate hydrate, **H2·H_2O**; stronger basic conditions employing sodium hydroxide in ethanol–water at pH ≈ 9–10 yield the new diphthalamate, **$Na_2$3·3H_2O**. Strongly basic conditions (*e.g.* pH ⩾ 11) do not lead to significant hydrolysis of the phthalimide moiety.

Elemental analysis, IR and NMR spectra are consistent with these formulations (Experimental section). The FAB mass spectrum of **H2·H_2O** is dominated by peaks at $m/z = 763$ ($[(\mathbf{H2})_2 + H]^+$), 400 ($[\mathbf{H2}\cdot H_2O + H]^+$) and 382 ($[\mathbf{H2} + H]^+$) while that of **$Na_2$3·3$H_2O$** features peaks at $m/z = 400$ ($[\mathbf{H_3 3}]^+$), 422 ($[\mathbf{NaH_2 3}]^+$), 444 ($[\mathbf{Na_2 H3}]^+$), 466 ($[\mathbf{Na_3 3}]^+$). There are also peaks due to dimers at $m/z = 799.4$ ($[\mathbf{H_5(3)_2}]^+$), 843.3 ($[\mathbf{Na_2 H_3(3)_2}]^+$), 865.3 ($[\mathbf{Na_3 H_2(3)_2}]^+$), 887 ($[\mathbf{Na_4 H(3)_2}]^+$), 909 ($[\mathbf{Na_5(3)_2}]^+$), and trimers with $m/z = 1265$ ($[\mathbf{Na_3 H_4(3)_3}]^+$), 1287 ($[\mathbf{Na_4 H_3(3)_3}]^+$), 1309 ($[\mathbf{Na_5 H_2(3)_3}]^+$), 1331 ($[\mathbf{Na_6 H(3)_3}]^+$), 1353 ($[\mathbf{Na_7(3)_3}]^+$). The ease with which **H2** and **$Na_2$3** dimerise and/or trimerise in the FABMS analyses is indicative of the presence of relatively strong non-covalent intermolecular interactions. Since these interactions (especially π–π and other stacking interactions) are of primary interest as potential conduits for electronic energy, verification of their presence and better understanding of their nature are required. For this reason and the need for conclusive evidence for the success of the hydro-

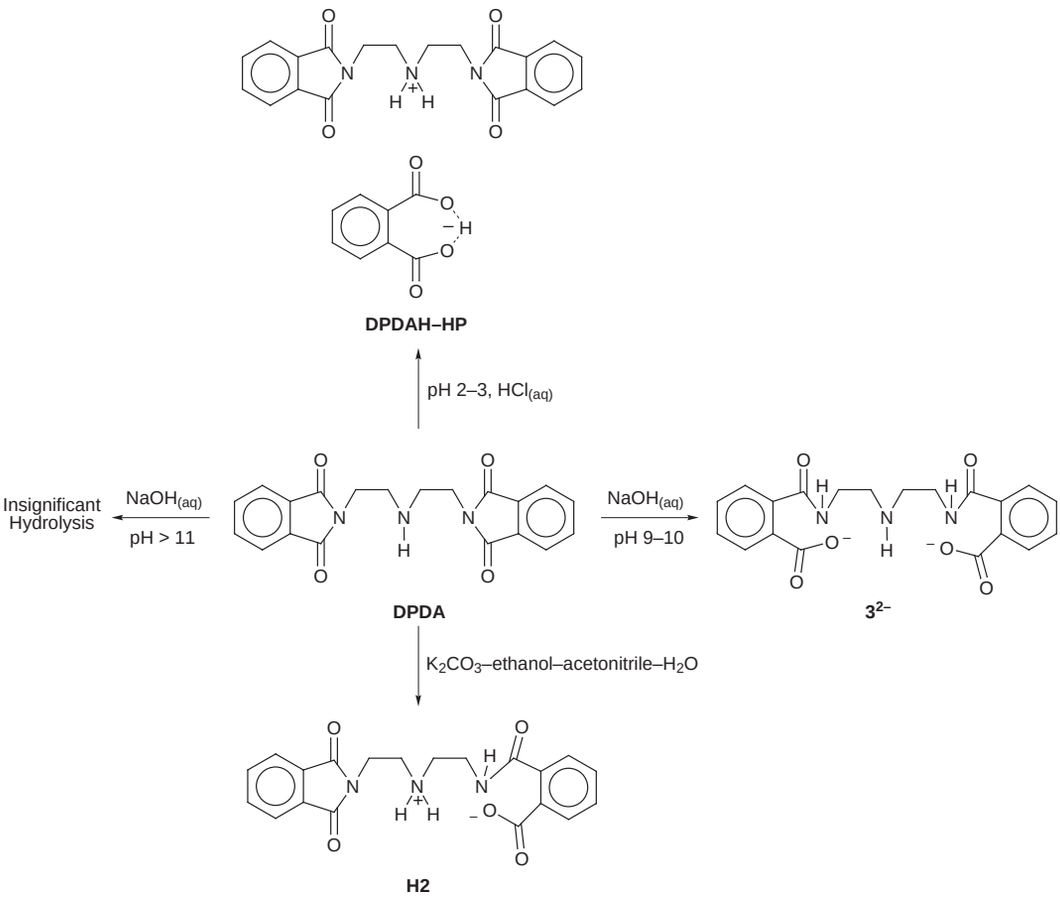

Scheme 1 Hydrolysis of DPDA

Table 1 Crystal data

Compound	**H2·H$_2$O**	**DPDAH–HP·1.75H$_2$O**
Chemical formula	$C_{20}H_{19}N_3O_5\cdot H_2O$	$C_{28}H_{23}N_3O_8\cdot 1.75H_2O$
Crystal system	Triclinic	Monoclinic
Space group	$P\bar{1}$	$P2_1/n$
a/Å	8.8221(2)	13.6174(6)
b/Å	8.9664(3)	11.3460(5)
c/Å	13.9424(5)	17.2252(9)
α/°	93.734(3)	90
β/°	92.092(5)	91.189(4)
γ/°	119.087(3)	90
V/Å^3	958.80(5)	2660.8(9)
Z	2	4
d_c/g cm^{-3}	1.383	1.400
μ(Cu-Kα)/cm^{-1}	8.67	9.05
T/K	293(2)	293(2)
Crystal size/mm^3	0.31 × 0.31 × 0.27	0.32 × 0.30 × 0.20
Reflections measured	2941	4381
θ Range/°	6.36–59.98	4.10–61.99
Reflections observed [$I > 2\sigma(I)$]	2619	3350
Parameters refined	275	382
R_1	0.0382	0.0434
wR_2	0.0997	0.1076

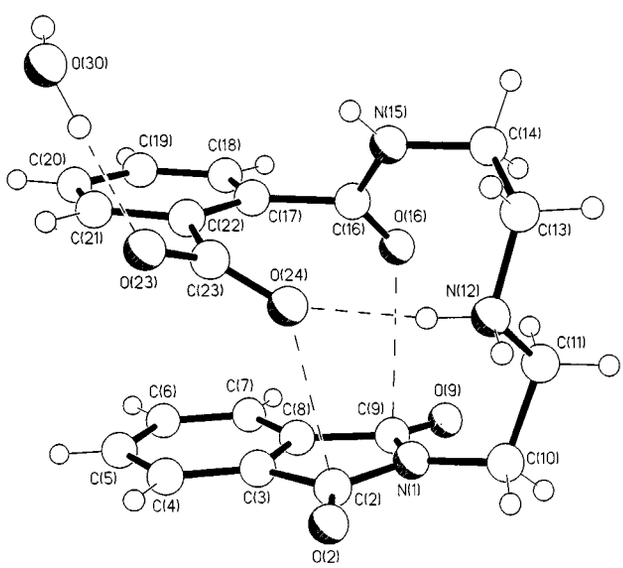

Fig. 1 Molecular structure of **H2·H$_2$O** showing the intermolecular hydrogen bonding and carbonyl–carbonyl interactions. Hydrogen bonding geometries: N···O 2.78 Å, H···O 1.93 Å; N–H···O angle 156°; O···O 2.73 Å, H···O 1.85 Å, O–H···O angle 177°.

lytic manipulations (Scheme 1) single crystal X-ray diffraction analyses of the crystalline products **H2·H$_2$O** and **DPDAH–HP·1.75H$_2$O** were undertaken.

Essential crystal data are shown in Table 1, while atomic positions, bond distances and angles and other structural data are available as supplementary material. The X-ray analysis shows conclusively that partial hydrolysis of **DPDA** was successful under mildly basic conditions. Phthalamate **H2** in **H2·H$_2$O** has a folded conformation (Fig. 1) with the benzoate group positioned above and almost parallel to the phthalimide functionality; the π–π stacking separation (3.91 Å) is too long for any significant interaction. The principal intramolecular stabilizing interactions are (i) N–H···O hydrogen bond (2.78 Å) between one of the amino N–H groups and the carboxylate carbonyl [O(24)]; (ii) a pair of strong electrostatic carbonyl···carbonyl interactions between, in one case, the carboxylate oxygen [O(24)] and the phthalimide carbonyl carbon C(2) (2.92 Å) and in the other, between the amide oxygen O(16) and the other phthalimide carbonyl carbon C(9) (2.90 Å). In both instances of (ii), the approaches of the carbonyl oxygen atoms to the phthalimide carbonyl groups are nearly orthogonal.

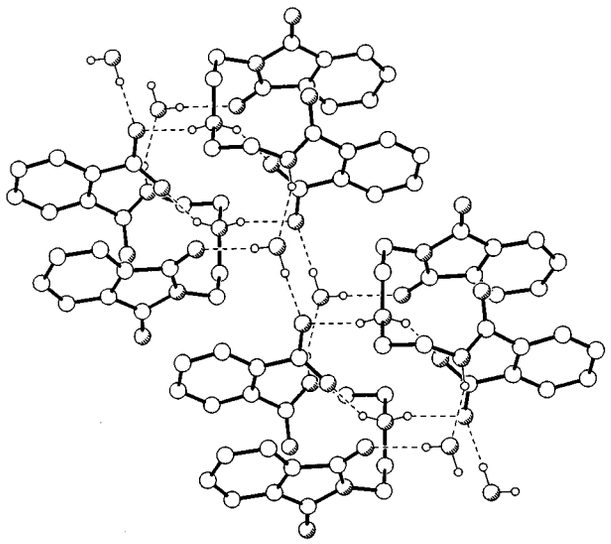

Fig. 2 Centrosymmetrically related hydrogen bonded 'dimer pairs' of **H2·H$_2$O** N(amine)···O(carboxylate) 2.71 Å, H···O 1.87 Å, N–H···O angle 154°; N(amido)···O(water) 2.83 Å, H···O 1.99 Å; N–H···O angle 156°; O(water)···O(phthalimido) 2.84 Å, H···O 1.98 Å, O–H···O angle 159°

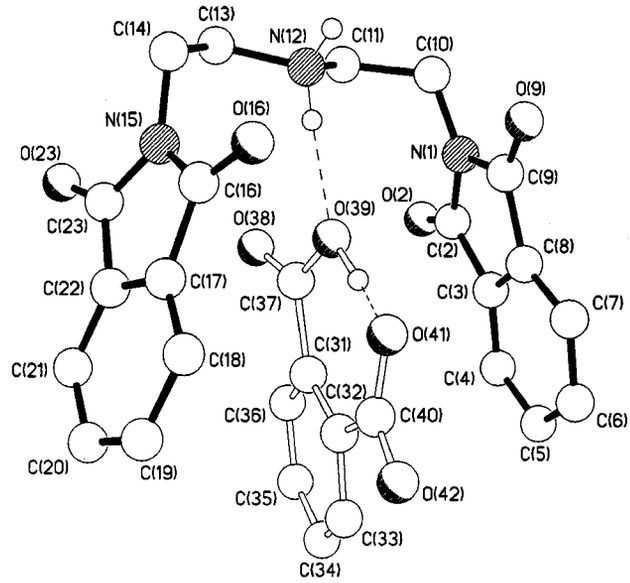

Fig. 3 Horseshoe conformation of **DPDAH**$^+$ and the trapped hydrogen phthalate anion in **DPDAH–HP·1.75H$_2$O**

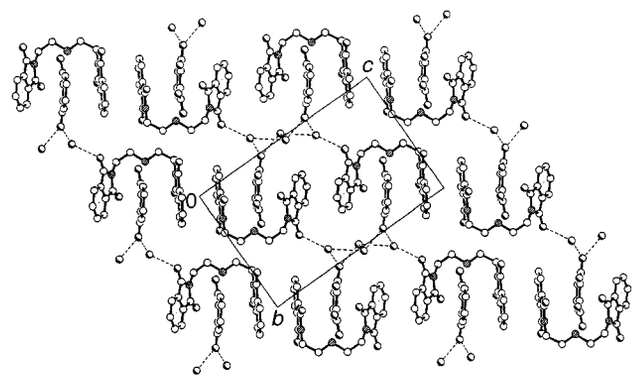

Fig. 4 Extended H-bonding in **DPDAH–HP·1.75H$_2$O** leading to a layer motif

Within the crystal, centrosymmetrically related pairs of molecules are linked *via* a pair of N–H···O H-bonds between the amino N–H hydrogen atom (not involved in intramolecular hydrogen bonding) of one molecule and one of the carboxylate oxygens [O(23)] of another and *vice versa* (Fig. 2). These molecules are further linked *via* hydrogen bonds between the amide N–H and the included water molecule and between this water molecule and one of the phthalimide carbonyl oxygen atoms. These hydrogen bonded 'dimer pairs' are further linked *via* the included water molecule to form chains that extend in the crystallographic *a* direction (Fig. 2). Thus, the appearance of the dimeric units $[(\mathbf{H2})_2 + H]^+$ in the FABMS of **H2·H$_2$O** is consistent with the presence of strong non covalent intermolecular interactions.

The X-ray analysis of the acid catalyzed hydrolytic product reveals, as expected,[17,18] that hydrolysis of **DPDA** at low pH is more effective than the base promoted reaction. In this case phthalic acid is produced and upon interaction with **DPDA** a stable complex, **DPDAH–HP·1.75H$_2$O** is formed. In the anhydrous **DPDAH–HP** described previously,[12] the molecule adapts an extended conformation with a mixture of *gauche* and *anti* geometries for the $CH_2CH_2N^+H_2CH_2CH_2$ backbone with the hydrogen isophthalate unit sandwiched between phthalimide groups of adjacent **DPDA** molecules (See Figs. 3, 5 and 6 in ref. 12). In sharp contrast, in the hydrated **DPDAH–HP·1.75H$_2$O** compound, the **DPDA** moiety is a host featuring a horseshoe conformation with an *all anti* geometry for its $CH_2CH_2N^+H_2CH_2CH_2$ linkage; the hydrogen isophthalate unit, being a guest, and inserted into the cleft formed by the two phthalimide rings (Fig. 3). Stabilization of the resulting supramolecular complex is achieved *via* a combination of (i) π–π stacking interactions between the hydrogen phthalate and one of the phthalimide [N(1)–C(9)] rings (mean planar separation 3.49 Å; centroid–centroid separation from the C(3)–C(8) ring 3.99 Å; rings inclined by *ca.* 6°) and (ii) N–H···O hydrogen bonding between one of the **DPDAH** aminium hydrogen atoms and one of the hydroxy oxygen atoms, O(39) of the hydrogen isophthalate (N···O, H···O distances 2.85, 1.95 Å, N–H···O angle, 176°). It is interesting to note that the 'bite' of the **DPDAH**$^+$ aromatic components is not enough to achieve simultaneous π–π stacking between both phthalimido rings and the trapped hydrogen isophthalate, the centroid–centroid separation between the C(31)–C(36) and C(17)–C(22) rings being 4.46 Å. The hydrogen isophthalate has, characteristically, a very short intramolecular O–H···O hydrogen bond of 2.39 Å which would normally be expected to be symmetric.[12,19] The X-ray evidence, however, indicates a noticeable asymmetry in the positioning of the hydrogen atom; the hydrogen position was refined isotropically and unconstrained. The O(39)–H and H···O(41) distances are 1.11(3) and 1.28(3) Å respectively; the associated O–H···O angle is 176°. An interesting consequence of this short H-bond coupled with a retention of near co-planarity of the carboxylate groups with the phenyl ring is an appreciable distortion of the sp^2 geometries at C(31) and C(32), the C(31)–C(32)–C(40) and C(37)–C(31)–C(32) angles being *enlarged* to 127.7(2) and 129.2(2)° respectively, *i.e.* the oxygen atoms O(39) and O(41) being unable to approach any closer.

Investigations of the packing of the 1:1 **DPDAH–HP** complexes reveal the formation of an extended stack structure (Fig. 4) with both phthalimido rings being stacked with C_i related counterparts. The degree of overlap of each ring differs within the case of the N(1)–C(9) ring, there being almost total head-to-tail overlap with the mean inter-planar separation of 3.37 Å, while for the N(15)–C(23) ring only the phenyl rings overlay each other—mean inter-planar separation 3.38 Å. In one direction the stacks are co-directional with adjacent chains approximately *anti*-phase to each other and they are cross-linked *via* H-bonds between one of the hydrogen phthalate carbonyl oxygen atoms and the included water molecules to form a sheet that extends within the 011 plane. Symmetry related sheets in the crystallographic *a* direction are parallel but have their π–π stacking directions inclined by *ca.* 65°. Adjacent

sheets are cross-linked *via* additional hydrogen bonds involving this time the aminium N–H hydrogen atom (not involved in intramolecular hydrogen bonding) and the included water molecules.

Lanthanide(III) complexes

DPDA itself turned out to be a very poor binder for Ln^{3+} ions, therefore complexes of the new chelates $\mathbf{2}^-$ and $\mathbf{3}^{2-}$, the preparations of which were inspired by the potential for the phthalamate anion to chelate lanthanide(III) ions and sensitize intense green $Tb^{3+}(^5D_4)$ and red $Eu^{3+}(^5D_0)$ emission, were of greater interest. Preliminary luminescence experiments revealed that the new monophthalamic acid (**H2**), and phthalimides generally, exhibit broad white light emission which overlaps many lanthanide f–f absorptions in the region 400–600 nm and therefore meet a crucial Förster–Dexter requirement for ligand-to-metal energy transfer.[20] It was therefore interesting to prepare compounds of Ln^{3+} ions (Eu^{3+} and Tb^{3+}) with phthalamates **H2** and $\mathbf{Na_2 3{\cdot}3H_2O}$ and study their electronic properties in order to determine whether compounds featuring beneficial electronic coupling leading to efficient ligand-to-Ln^{3+} energy transfer and subsequent intense sensitized Ln^{3+} emission can be so derived.

The europium(III) compound of **H2** was isolated as pale thick irregularly shaped crystals with the stoichiometry $Ln(\mathbf{H2})_3(NO_3)_3{\cdot}2H_2O$ (**4**), based on elemental analysis; efforts to grow good crystals of suitable quality for single crystal X-ray diffraction analyses were not successful. FABMS of **4** is consistent with the above formulation and indicates that the compound is unstable under FABMS conditions. Products of its extensive fragmentation include **H2**: $m/z = 382$ ($[\mathbf{H2} + H]^+$) and 763 ($[(\mathbf{H2})_2 + H]^+$), both of which were seen in the FABMS of the parent phthalimide–phthalamate, $\mathbf{H2{\cdot}H_2O}$ (*vide supra*). It would seem, from the stoichiometry of **4** and its instability, that only the carboxylate anionic site of zwitterionic **H2** binds the Ln^{3+} cation. For this reason and the low yields of **H2**, we turned to diphthalamate $\mathbf{Na_2 3{\cdot}3H_2O}$ for which the two carboxylate moieties are likely to bind the lanthanide ions more strongly.[12]

Europium(III) and terbium(III) complexes of $\mathbf{3}^{2-}$ are readily obtained from a water–ethanol mixture as insoluble powders having the stoichiometry $Ln_2\mathbf{3}(OH)_3(OCH_3)$, Ln = Eu (**5**), $Ln_2\mathbf{3}(OH)_2(OCH_3)_2$, Ln = Gd (**6**) and Tb (**7**). Efforts to grow crystals of **5**–**7** suitable for single crystal X-ray analyses were unsuccessful. Even the larger lanthanide(III) ions formed insoluble powders of the stoichiometry $Ln_2\mathbf{3}(OH)_3(OCH_3)$, Ln = La (**8**) and Pr (**9**) while neodymium formed the compound $NdNa\mathbf{3}(OH)_2$ (**10**).

Lanthanide(III) luminescence spectra and decay dynamics

Even though the coordination details of **4**–**10** are still unresolved, it is possible and indeed important to seek to obtain clues regarding the potential effectiveness of the phthalamate functionality in **H2** and $\mathbf{3}^{2-}$ as '*antenna groups*' for lanthanide(III) ions. We thus studied the luminescence behaviour of europium(III) (**4** and **5**) and terbium(III) (**7**) compounds of **H2** and $\mathbf{3}^{2-}$ to explore the potential of the phthalamate moiety to serve as a building block for new photonic devices.

Compound **4** emits visible intense red light at 615 nm [Fig. 5(a)] following excitation into the ligand states at about 300 nm for both 300 and 77 K. The excitation spectrum [Fig. 5(b)] is dominated by broad **H2** absorptions onto which typically weak sharp europium(III) absorptions are superimposed. Direct laser excitation of Eu^{3+} electronic states leads to very weak emission, which shows that **H2** is responsible for sensitizing most of the observed intense red europium emission. Peaks in the emission spectrum [Fig. 5(a)] are typically those of $Eu^{3+}(^5D_0)$ in moderately low symmetry. Remarkably, quenching processes in **4** are so inefficient that emission from the $Eu^{3+}(^5D_1)$ state (which is

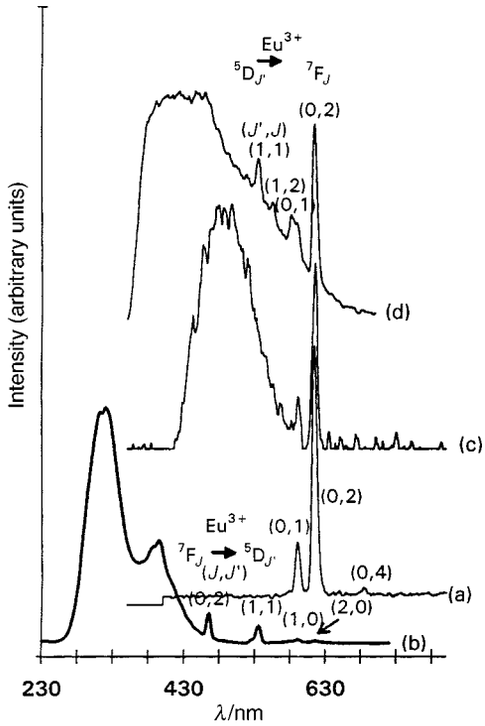

Fig. 5 Luminescence and excitation spectra of $Eu(\mathbf{H2})_3(NO_3)_3{\cdot}2H_2O$ (**4**): (a) emission spectrum (300 K); $\lambda_{exc} = 300$ nm, gating time $t_g = 1$ ms, delay time $t_d = 1$ ms; (b) excitation spectrum (300 K); $\lambda_{em} = 610$ nm $[Eu^{3+}(^5D_0)]$, $t_g = 1$ ms, $t_d = 1$ ms; (c) emission spectrum (77 K); $\lambda_{exc} = 300$ nm, $t_g = 1$ ms, $t_d = 12$ ms; (d) emission spectrum (77 K); $\lambda_{exc} = 300$ nm, $t_g = 0.01$ ms, $t_d = 0.02$ ms

normally very readily quenched *via* multiphoton relaxation processes[21a]) is also observed (even at low temperature). This emission is most evident in the time resolved spectra (TRS) recorded using comparatively short delay (20 μs) and gating (10 μs) times of the LS5 spectrometer [compare Fig. 5(c) and 5(d) and emission lifetimes: $Eu^{3+}(^5D_1)$, ≈10 μs; $Eu^{3+}(^5D_0)$, ≈500 μs]. Such good luminescence features are a hallmark of inorganic phosphors such as $Y_{0.95}Eu_{0.05}VO_4$ in which quenching due to molecular and lattice vibrations is minimal.[21b] Thermalized quenching of Ln^{3+} emission by vibrational or electronic states of organic fragments has generally been a serious limitation in the development of sensitized Ln^{3+} photonic devices based on organochromophores.[22,23] Therefore the temperature independent emission behaviour of Ln^{3+} bound to phthalamates could be an important breakthrough worth detailed exploration.

In order to determine whether the origin of the efficient '*antenna effect*' exhibited by **H2** is the phthalamate or phthalimide functionality we studied the luminescence behaviour of compounds (**5**, **7**) of the bis-phthalamate $\mathbf{3}^{2-}$. Both Eu^{3+} and Tb^{3+} emit strongly upon excitation into the broad phthalamate ligand absorption at *ca.* 300 nm. While the emission of **5** and **7** is due to metal ion transitions, the broad ligand absorption at *ca.* 300 nm and its shoulder at roughly 400 nm feature prominently in the corresponding excitation spectra (Figs. 6 and 7). Since the excitation spectra of Eu^{3+} emission from **4** and **5** are essentially similar, the observed '*antenna effect*' exhibited by chelates **H2** and $\mathbf{3}^{2-}$ is in both cases due to the phthalamate functionality.

Consistent with the above spectral observation, the emission intensity and decay rates of $Eu^{3+}(^5D_0)$ emission in **4** are essentially temperature independent; the decay rates are 1.9×10^3 and 2.1×10^3 s^{-1} at 77 and 300 K respectively following initial excitation buildups of roughly 3×10^5 (77 K) and 5.6×10^5 s^{-1} (300 K). The $Eu^{3+}(^5D_1)$ emission, monitored at 533 nm, follows non-exponential decay kinetics at 77 K but the decay rates of both the slow and fast components are roughly 10^5 s^{-1}. At 300 K this $Eu^{3+}(^5D_1)$ emission is exponential and decays at 3.7×10^5

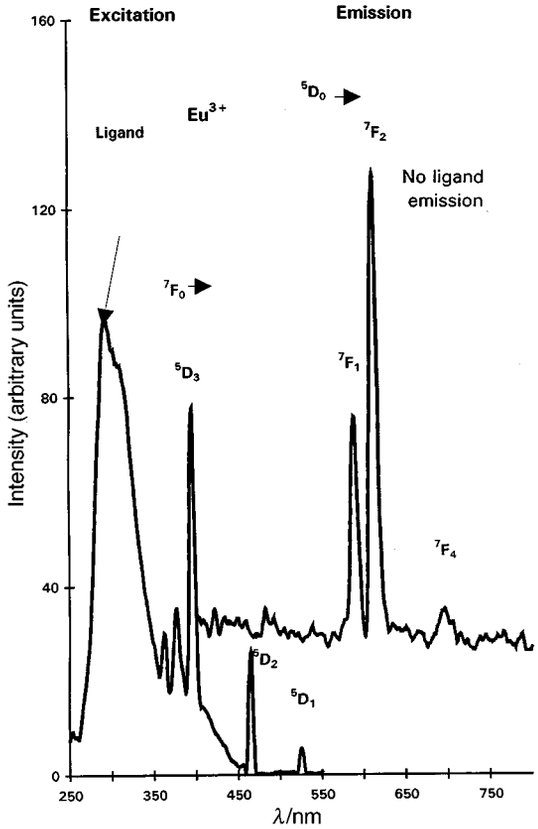

Fig. 6 77 K (λ_{exc} = 300 nm) and excitation (λ_{em} = 610 nm) spectra of **5**

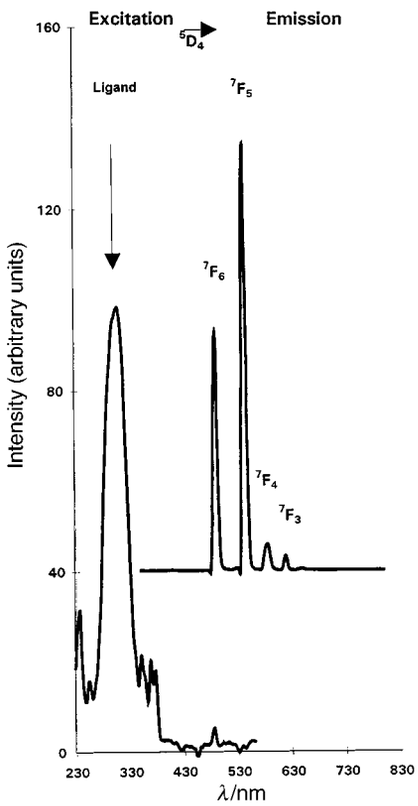

Fig. 7 77 K (λ_{exc} = 300 nm) and excitation (λ_{em} = 540 nm) spectra of **7**

s^{-1}. These decay rates of the $Eu^{3+}(^5D_1)$ state are similar in magnitude to the excitation buildup rates of the red $Eu^{3+}(^5D_0)$ emission. This feature and the occurrence of the $^5D_1 \leftarrow {}^7F_J$ transitions in the excitation spectrum of the $Eu^{3+}(^5D_0)$ emission indicate that the $Eu^{3+}(^5D_1)$ state in **4** is quenched by internal conversion to the lower $Eu^{3+}(^5D_0)$ state. Further, **H2**-to-Eu^{3+} energy transfer appears to be efficient and fast compared to the timescale limits of our measurements (roughly 0.1 μs).

The emission and excitation spectral profiles of crystalline **H2·H$_2$O** are similar to those of **H2** in **4** [emission TRS shows short and long lived components at $\lambda_{max} \approx 410$ and 480 nm respectively (Fig. 5)]. But the 77 K decay rates (7 s^{-1} for the slow parts) of crystalline **H2** are slower [compare to a decay rate of the long lived component (≈12 s^{-1}) for **H2** in **4**]. Ligand emission in **4** is much weaker compared to that of $Eu^{3+}(^5D_0)$ [Fig. 5(a)].

The luminescence decay curves of $Eu^{3+}(^5D_0)$ (λ_{exc} = 337 nm, λ_{em} = 613 nm) in **5** show rises of *ca.* 9×10^4 (77 K) and 3.6×10^5 s^{-1} (300 K) followed by nearly exponential and marginally temperature dependent decay (rate ≈3×10^3 s^{-1}). Again the quenching processes are so inefficient that $Eu^{3+}(^5D_1)$ emission is also observed even at room temperature [decay kinetics are complicated but rates are of the order of 1×10^6 (300 K) and 1×10^5 (77 K) s^{-1}]. The rise rates of $Eu^{3+}(^5D_0)$ emission and the fast decay components of $Eu^{3+}(^5D_1)$ are of similar magnitude and $^5D_1 \leftarrow {}^7F_J$ absorptions are found in the excitation spectrum of the $Eu^{3+}(^5D_0)$ emission (Fig. 6). We thus attribute the rise on the decay curve of the $Eu^{3+}(^5D_0)$ emission to internal conversion from the upper $Eu^{3+}(^5D_1)$ state. Ligand-to-Eu^{3+} energy transfer again appears to be too fast to measure on our system. The luminescence of $Tb^{3+}(^5D_4)$ in **7** (λ_{exc} = 337 nm; emission monitored at λ_{em} = 613 nm to minimize ligand interference) at 77 K shows a rise of *ca.* 8×10^4 s^{-1} and is followed by exponential decay at *ca.* 1×10^3 s^{-1}. At 300 K the decay process is not exponential but the tail decays at *ca.* 1×10^3 s^{-1}. These results suggest that the $Tb^{3+}(^5D_4)$ emission is somewhat quenched at room temperature.

Conclusion

We conclude that the phthalamate functionality of **H2** and $\mathbf{3}^{2-}$ is an efficient sensitizer for visibly strong $Eu^{3+}(^5D_0)$ and Tb^{3+}-$(^5D_4)$ emission and remarkably the desirable '*antenna effect*' is achieved without the usual[22,23] active temperature dependent quenching processes for $Eu^{3+}(^5D_0)$; for $Tb^{3+}(^5D_4)$, some quenching is observable at room temperature. Frequently, the desirable strong coupling between the ligand and Ln^{3+} electronic states leads to two dichotomous effects: strong sensitization of Ln^{3+} emission, usually at low temperature (*e.g.* 77 K), and quenching of this emission at room temperature through efficient thermally activated metal-to-ligand back energy transfer.[22–24] The above encouraging results, in which ligand-to-metal energy transfer remains faster and more efficient than quenching processes, reveal the attractiveness of phthalamate moieties as potentially new types of building blocks for photonic devices.

Experimental

Elemental analyses

Carbon, hydrogen and nitrogen were obtained from MEDAC Ltd., Brunel University, Uxbridge, UK.

Spectral measurements

Routine IR and ^{1}H NMR spectra were acquired from the Perkin-Elmer 1600 FTIR and Bruker ACE200 spectrometers described earlier.[12] 500 MHz NMR spectra were obtained at Cambridge University using a DRX500 spectrometer. Fast atom bombardment mass spectra were obtained using AutoSpecQ (Imperial College) or Kratos MS50 (Cambridge University) instruments. The Perkin-Elmer LS5 luminescence spectrometer and the nitrogen laser set used to acquire decay curves were described previously.[25]

Preparations

H2·H$_2$O. Solid **DPDA** suspended in a mixture of ethanol and

dichloroethane containing about five drops of water was stirred at 50 °C for one week. The mixture was then filtered and slow evaporation of the filtrate yielded clear crystals of **H2·H_2O** in about 10% yield (Found: C, 60.65; H, 5.39; N, 10.24%. $C_{20}H_{21}N_3O_6$ requires C, 60.1; H, 5.3; N, 10.5). δ_H(500 MHz) 3.24 (m), 3.92 (m), 7.46 (m), 7.75 (s), 7.95 (m).

Eu(H2)$_3$(NO$_3$)$_3$·2H_2O (4). The complex was prepared by reacting Eu(NO$_3$)$_3$·*n*H_2O (1 mmol) with **H2·H_2O** (0.3 mmol) in ethanol. Slow evaporation of the resulting solution yielded **Eu(H2)$_3$(NO$_3$)$_3$·2H_2O** as pale yellow thick irregular crystals which gradually become wet when exposed to the atmosphere (yield ≈16%) (Found: C, 47.49; H, 4.02; N, 11.08%. C_{60}-$EuH_{60}N_{12}O_{26}$ requires C, 47.4; H, 4.0; N, 11.1).

$Na_2$3·3H_2O. One mmol of DPDA was suspended in 100 cm^3 ethanol and 2 mmol sodium hydroxide in 10 cm^3 of water were added. The suspension was stirred at room temperature and maintained at about pH 9 and then refluxed for 1 h. Upon cooling the solution yielded the salt as a white powder in almost quantitative yield (Found: C, 48.70; H, 5.35; N, 8.50%. $C_{20}H_{25}$-$N_3Na_2O_9$ requires C, 48.3; H, 5.1; N, 8.5). δ_H(200 MHz; D_2O): 3.41 (4H, t), 3.74 (4H, t), 7.37–7.61 (8H, m). δ_C 41.47, 48.94, 129.48, 130.74, 131.91, 132.74, 137.82, 175.91, 178.22. The hydrogen chloride salt, **[$H_2$3·HCl]·0.5H_2O**, was obtained as small needles by recrystallizing the sodium salt **$Na_2$3·3H_2O** from a hydrochloric acid solution of pH ≈ 2.5 (Found: C, 54.29; H, 5.05; N, 9.49%. $C_{20}ClH_{22}N_3O_{6.5}$ requires C, 54.0; H, 5.2; N, 9.5).

Lanthanide(III) complexes of 3^{2-}. 1.5 mmol of **$Na_2$3·3H_2O** were dissolved in 150 cm^3 of water and 3 mmol of lanthanide (III) nitrates dissolved in 50 cm^3 of methanol were added. The resulting solution was evaporated slowly until a white precipitate was deposited. Once deposited the compounds are insoluble in water (yield ≈ 18–68%). [**5**: Found: C, 32.47; H, 3.42; N, 5.28%. $C_{21}Eu_2H_{25}N_3O_{10}$ requires: C, 32.2; H, 3.2; N, 5.4. **6**: Found: C, 32.44; H, 3.42; N, 5.28%. $C_{22}Gd_2H_{27}N_3O_{10}$ requires C, 32.7; H, 3.4; N, 5.2. **8**: Found: C, 32.08; H, 3.29; N, 4.93%. $C_{21}H_{25}La_2N_3O_{10}$ requires: C, 32.2; H, 3.2; N, 5.4. **9** (as **9·H_2O**): Found: C, 32.40; H, 3.39; N, 4.29%. $C_{21}H_{27}N_3O_{11}Pr_2$ requires: C, 32.4; H, 3.5; N, 5.4. **10** (as **10·H_2O**): Found: C, 38.68; H, 3.86; N, 6.84%. $C_{20}H_{23}N_3NaNdO_9$ requires: C, 38.96; H, 3.8; N, 6.8].

Crystallography

Data for **H2·H_2O** were measured on a Siemens P4/RA diffractometer and for **DPDAH–HP·1.75H_2O** on a Siemens P4/PC diffractometer; in both cases graphite-monochromated Cu-Kα radiation and ω scans were used. The structures were solved by direct methods and the non-hydrogen atoms refined anisotropically using full matrix least squares[26] based on F^2.

Atomic coordinates, bond distances and angles, thermal parameters have been deposited at the Cambridge Data Centre. For details of the deposition scheme, see 'Instructions for Authors', *J. Chem. Soc.*, *Perkin Trans. 2*, available *via* the RSC Web page (http://www.rsc.org/authors). Any request to the CCDC for this material should quote the full literature citation and the reference number 188/133.

Acknowledgements

We thank the Leverhulme Trust (grant F/709A), Schering Ag and the InterAmerican Development Bank (Grant R&D #29) for supporting the work at the University of the West Indies (UWI) as well as the UWI–British Council CICHE programme for supporting the UWI–Imperial College link. We are also grateful to P. Grice and S. V. Ley (Cambridge University) for assistance with high field NMR and FABMS and the Forensic Laboratory (Jamaica) for a loan of the LS5 spectrometer.

References

1 (*a*) R. C. Howell, K. V. N. Spence, A. J. P. White and D. J. Williams, *J. Chem. Soc.*, *Dalton Trans.*, 1996, 961 and references therein; (*b*) I. A. Kahwa, S. Folkes, D. J. Williams, S. V. Ley, C. A. O'Mahoney and G. L. McPherson, *J. Chem. Soc.*, *Chem. Commun.*, 1989, 1531; (*c*) K. D. Matthews, S. Bailey-Folkes, I. A. Kahwa, G. L. McPherson, C. A. O'Mahoney, S. V. Ley, D. J. Williams, C. J. Goombridge and C. J. O'Connor, *J. Phys. Chem.*, 1992, **96**, 7021.
2 P. R. Selvin, J. Jancarik, M. Li and L.-W. Hung, *Inorg. Chem.*, 1996, **34**, 700.
3 A. Døssing, H. Toftlund, A. Hazell, J. Bourssa and P. C. Ford, *J. Chem. Soc.*, *Dalton Trans.*, 1997, 355.
4 C. Pigeut, J.-C. G. Bünzli, G. Bernardinelli, G. Hopfagartner, S. Petoud and O. Schaad, *J. Am. Chem. Soc.*, 1996, **118**, 6681.
5 Z. Wang, J. Reibenspies and A. E. Martell, *Inorg. Chem.*, 1997, **36**, 629.
6 C. Piguet, G. Hopfagartner, A. F. Williams and J.-C. G. Bünzli, *J. Chem. Soc.*, *Chem. Commun.*, 1995, 491.
7 C. Pigeut, G. Bernardinelli, J.-C. G. Bünzli, S. Petoud and G. Hopfagartner, *J. Chem. Soc.*, *Chem. Commun.*, 1995, 2575.
8 N. Sabbatini, M. Guardigli and J.-M. Lehn, *Coord. Chem. Rev.*, 1993, **123**, 201.
9 L. Fabbrizz and A. Poggi, *Chem. Soc. Rev.*, 1995, **24**, 197.
10 V. Balzani and F. Scandola, *Supramolecular Photochemistry*, Ellis Horwood, Chichester, 1991.
11 S. F. Mason, *Mol. Phys.*, 1975, **30**, 1829; S. P. Sinha and E. Butter, *Mol. Phys.*, 1969, **16**, 285; B. R. Judd, *Phys. Rev.*, 1973, **10**, 195; G. S. Ofelt, *J. Chem. Phys.*, 1962, **37**, 511; J. H. Försberg, *Coord. Chem. Rev.*, 1973, **10**, 195; J.-C. G. Bünzli, in *Lanthanide Probes in Life*, *Chemical and Earth Sciences*, ed. J.-C. G. Bünzli and G. R. Choppin, Elsevier, Amsterdam, 1989, p. 219; C. Fouassier, in *Encyclopaedia of Inorganic Chemistry*, ed. R. B. King, Wiley, New York, 1994, p. 1984.
12 D. M. Y. Barrett, I. A. Kahwa, G. L. McPherson and J. T. Mague, *J. Org. Chem.*, 1995, **60**, 5946.
13 D. M. Y. Barrett, I. A. Kahwa and D. J. Williams, *Acta. Crystallogr.*, *Sect. C*, 1996, **52**, 2069.
14 J. W. Burlow, R. S. Davidson, A. Lewis and D. R. Russell, *J. Chem. Soc.*, *Perkin Trans. 2*, 1997, 1103.
15 G. H. Dieke, *Spectra and energy levels of rare earth ions in crystals*, Interscience, New York, 1968.
16 D. Parker, *Chem. Soc. Rev.*, 1990, **19**, 271; P. Gueirriero, J. Tamburini and P. A. Vigato, *Coord. Chem. Rev.*, 1995, **139**, 17.
17 J. D. Doyle, A. Harriman and G. L. Newport, *J. Chem. Soc.*, *Perkin Trans. 2*, 1979, 799.
18 B. Zerner and M. L. Bender, *J. Am. Chem. Soc.*, 1961, **83**, 2267.
19 H. Kuppers, *Z. Kristallogr.*, 1990, **192**, 97.
20 L. Dexter, *J. Chem. Phys.*, 1953, **21**, 836; Th. Förster, *Ann. Phys.* (*Leipzig*), 1948, **2**, 55.
21 (*a*) R. Reinsfield and C.-K. Jörgensen, *Inorganic Concepts 1. Lasers and Excited States of Rare Earths*, Springer-Verlag, Berlin, 1977; (*b*) J. Loriers, J. P. Denis and J. P. Briffant, *C. R. Acad. Sci. Paris*, *Ser. B*, 1966, **262**, 496; A. K. Levin and F. C. Palilla, *Appl. Phys. Lett.*, 1964, **5**, 118; J. A. Baglio and G. Gashurov, *Acta. Crystallogr.*, *Sect. B*, 1968, **24**, 292.
22 K. D. Matthews, I. A. Kahwa and D. J. Williams, *Inorg. Chem.*, 1994, **33**, 1382.
23 B. Alpha, R. Ballardini, V. Balzani, J.-M. Lehn, S. Perathoner and N. Sabbatini, *Photochem. Photobiol.*, 1990, **52**, 409.
24 R. C. Holz, G. E. Meister and W. deW. Horrocks, Jr., *Inorg. Chem.*, 1990, **29**, 5193.
25 R. A. Fairman, W. A. Gallimore, K. V. N. Spence and I. A. Kahwa, *Inorg. Chem.*, 1994, **33**, 823.
26 SHELXTL PC Release 5.03, Siemens Analytical X-Ray Instruments Inc., Madison, WI, 1994.

Paper 8/04356F
Received 9*th June* 1998
Accepted 10*th June* 1998